Myelin Instability and Oligodendrocyte Metabolism in Myelin-deficient Mutant Mice

Jean-Marie Matthieu, Jean-Marc Roch, François X. Omlin,* Isabel Rambaldi,‡ Guillermina Almazan, and Peter E. Braun‡

Laboratoire de Neurochimie, Service de Pédiatrie, Centre Hospitalier Universitaire Vaudois, *Institut d'Histologie et d'Embryologie de L'Université de Lausanne, Lausanne, Switzerland; and ‡Department of Biochemistry, McGill University, Montréal, Québec, Canada

Abstract. During the active phase of myelination in myelin-deficient mutant mice (*mld*), myelin basic protein (MBP) synthesis is defective and the myelin lamellae are uncompacted. In these mutants, we found a fast metabolism of the myelin-associated glycoprotein (MAG) and of sulfatides, and the presence of cholesterol esters and a degradation product of MAG, dMAG, indicating that *mld* myelin was unstable. The increased synthesis of MAG and Wolfgram protein, two proteins present in uncompacted myelin sheath and paranodal loops, was demonstrated by high levels of messengers. Simultaneously, we found an accumulation of inclusion bodies, vacuoles, and rough endoplasmic reticulum in *mld* oligodendrocytes. This material was heavily immunostained for MAG. Furthermore, the developmental change between the two molecular forms of MAG (p72MAG/p67MAG) was delayed in *mld* mice. In 85-d-old *mld* mice, the MBP content increased and myelin lamellae became better compacted. In these mutants, dMAG was absent and MAG mRNAs were found in normal amounts. Furthermore, the fine structure of *mld* oligodendrocytes was normal and the MAG immunostaining was similar to age-matched controls. These results support a functional role for MBP in maintaining the metabolic stability and the compact structure of myelin. Furthermore, in the absence of MBP and myelin compaction, the regulation of the synthesis of at least two membrane proteins related to myelin cannot proceed.

In the central nervous system of homozygous myelin-deficient mutant mice (*mld*)[1] that are affected by a severe myelin deficit (Doolittle and Schweikart, 1977), the major electron-dense line of myelin is absent and myelin basic protein (MBP) concentrations are drastically reduced (Bourre et al., 1980, Ginalski-Winkelmann et al., 1982, Matthieu et al., 1980a). MBP has been localized in the major dense line of compact central and peripheral myelin using immunocytochemical techniques at the electron microscopic level (Omlin et al., 1982), and it is generally accepted that MBP plays a key role in the fusion of the cytoplasmic faces of the oligodendroglial plasma membrane (Braun, 1984; Kirschner et al., 1984). Recently, we showed that when MBP concentration in central nervous system myelin of *mld* mutants increases after the active phase of myelin deposition is completed in controls, the major electron-dense line appears concomitantly, and myelin lamellae are better compacted (Matthieu et al., 1984b). The *mld* mutation affects the synthesis of MBP (Campagnoni et al., 1984; Ginalski-Winkelmann et al., 1983) whereas that of intrinsic myelin proteins is not reduced (Matthieu et al., 1984a).

Shiverer mice phenotype is similar to *mld* (Dupouey et al., 1979; Lachapelle et al., 1980; Matthieu et al., 1981) and cross-breeding experiments indicate that both mutants are alleles (Lachapelle et al., 1980). Although shiverer involves a deletion in the MBP gene (Kimura et al., 1985; Roach et al., 1983), we found it unlikely that the *mld* mutation involves a deletion in the coding region of the gene (Roch et al., 1986) as we were able to translate *mld* mRNA into MBP polypeptides, though in reduced amounts, with normal molecular masses and immunoreactivity.

The aim of this work was to investigate the stability of the myelin sheath in the absence of one of its major components, MBP, and to study the metabolism and regulation of other myelin components that are not affected by the *mld* mutation.

Preliminary progress reports of this study have appeared in abstract forms (Almazan et al., 1983; Matthieu et al., 1982; Matthieu and Omlin, 1985; Omlin and Matthieu, 1984).

Materials and Methods

Animals

The *mld* mice and unaffected littermates used as controls are direct descendants of 15 pairs of mice from stock obtained from Dr. P. Doolittle (School

1. *Abbreviations used in this paper*: MAG, myelin-associated glycoprotein; MBP, myelin basic protein; *mld*, myelin-deficient.

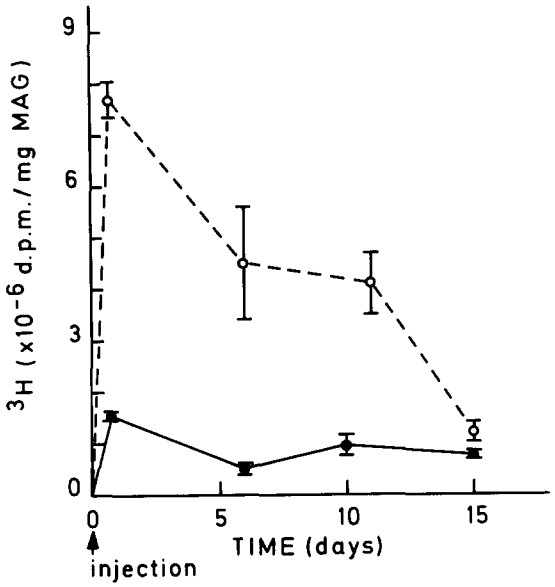

Figure 1. Metabolism of MAG labeled in vivo with [^{3}H]fucose. Normal littermates (*solid circle*) and *mld* mutants (*open circle*) were injected at 21 d of age and killed after 16 h and 6, 10, and 15 d. The results given as specific radioactivity in dpm are the mean for three to five separate animals given with the standard error of the mean. Similar results were obtained in 25- and 60-d-old animals.

of Agriculture, Purdue University, Lafayette, IN) in 1979. From the start the stock has been kept free from any out-cross and can be considered as inbred. For in vivo labelling, the mice were injected in each cerebral hemisphere, under ether anesthesia, with 10 μCi L-[5,6-^{3}H]fucose (40–60 Ci/mmol) or $Na_2{}^{35}SO_4$ (10–1,000 mCi/mmol sulfur; New England Nuclear, Boston, MA). The animals were killed by decapitation, the brains, optic nerves, and spinal cords were rapidly removed, rinsed in ice-cold isotonic saline, weighed, and stored at −80°C until myelin was isolated. For RNA isolation, the tissue was immediately frozen in liquid nitrogen after dissection and stored at −80°C.

Antisera

Polyclonal rabbit antisera to MBP, Wolfgram protein, and myelin-associated glycoprotein (MAG) have been prepared in our laboratory and characterized (Matthieu et al., 1984a, 1986; Waehneldt et al., 1985). The antiserum to the glial fibrillary acidic protein was a generous gift of Dr. L. F. Eng (Veterans Administration Medical Center, Palo Alto, CA).

Protein and Lipid Analysis

Frozen brains were homogenized in 0.32 M sucrose and myelin was isolated (Norton and Poduslo, 1973). Homogenate and myelin aliquots were removed and used for protein (Lowry et al., 1951), MAG (Johnson et al., 1982), and sulfatide (Kean, 1968) determination. Total lipids from *mld* and control brains at 25 d of age were extracted (Folch et al., 1957) and separated by thin layer chromatography to detect cholesterol esters (Kraus-Ruppert et al., 1972).

[^{35}S]Sulfatides were counted for radioactivity by liquid scintillation spectrometry. The incorporation of ^{3}H into MAG was measured after separation by SDS-PAGE as reported in detail elsewhere (Quarles et al., 1985).

Delipidated myelin fractions or nervous tissue homogenate samples were solubilized in SDS and separated by electrophoresis on polyacrylamide disc or slab gels (Laemmli, 1970). Proteins separated by electrophoresis were transferred electrophoretically to nitrocellulose sheets (Towbin et al., 1979). The nitrocellulose sheets were incubated successively with preimmune sera or antisera to MAG, then with ^{125}I-protein A (2–10 Ci/g, New England Nuclear, Boston, MA) and exposed to Kodak X-Omat AR-5 film at −80°C. Autoradiographs were scanned on a Vitatron TLD 100 densitometer measuring the transmitted light. Molecular masses of proteins were estimated from a graph of the logarithm of the molecular masses of standard molecules versus their migration distances on the gels.

Isolation of mRNA and Size Fractionation

Total RNA was prepared from mouse brains by phenolchloroform extraction and ethanol precipitation. It was then loaded onto an oligo-dT cellulose column in order to select the poly(A)$^+$ RNAs. In some experiments, mRNAs were size-fractionated by centrifugation on a sucrose gradient. These procedures are described in detail by Maniatis et al. (1982).

In Vitro Translation and Immunoprecipitation

In vitro translation of the poly(A)$^+$ RNAs was performed in a nuclease-treated message-dependent rabbit reticulocyte lysate (Amersham International, Amersham, England) in the presence of L-[^{35}S]methionine (1,300 Ci/mmol, Amersham International). We used 2 μg of mRNA with 14 μl lysate and 20 μCi L-[^{35}S]methionine in a total reaction volume of 20 μl. Protein synthesis was carried out for 1 h at 30°C. After a chase (2 μl of 10 mM cold L-methionine, 30 min at 30°C), the level of protein synthesis was estimated by TCA precipitation of 2-μl aliquots on glass fiber filters followed by liquid scintillation counting. The rest of each sample was then placed in boiling water for 5 min in the presence of 4% SDS, and diluted with 500 μl RIPA buffer (1% Triton X-100, 150 mM NaCl, 5 mM EDTA, 50 mM Tris HCl, pH 7.4). Equal amounts of synthesized proteins, as determined by TCA precipitation, were immunoprecipitated as follows: (*a*) preclearing for 2 h at room temperature with 30 μl of 10% *Staphylococcus aureus* cells (Calbiochem-Behring Corp., San Diego, CA), with stirring; (*b*) immunoreaction overnight at 4°C with 10 μl antiserum; and (*c*) immunoadsorption for 2 h at room temperature with 30 μl of 10% *S. aureus* cells, with stirring. The cells carrying immune complexes were washed three times with RIPA buffer before solubilization at 95°C for 5 min in 55 μl of sample buffer (150 mM Tris HCl, pH 6.8, 6% SDS, 6 mM EDTA, 0.03% bromophenol blue, 30% glycerol, 1% β-mercaptoethanol). The immunoprecipitated translation products were then separated by SDS-PAGE (8–15%) according to Laemmli (1970). After Coomassie Blue staining, the gel was treated with Na-salicylate and exposed for 18 d at −80°C on a Kodak film (X-Omat SO-282). The films were scanned on a densitometer for quantitative estimation.

Morphology

For light and electron microscopic investigations, mutant mice and unaffected littermates were studied at different stages of postnatal development: 7, 15, 30, 52, and 85 d after birth. For each age and group, four to six animals were fixed by intracardiac perfusion with a fixative containing 0.5% glutaraldehyde and 1.5% paraformaldehyde in 0.1 M phosphate buffer at pH 7.6. Optic nerves, cervical spinal cord, and trigeminal nerves were removed and cut into smaller pieces, which were postfixed in 2% osmium tetroxide for 2 h at room temperature and 1 h at 4°C. The samples were then dehydrated in ethanol and embedded in Epon. Thin sections were cut with a diamond knife on an Ultracut microtome (Reichert Scientific Instruments, Buffalo, NY), mounted on Formvar-coated slot grids, and examined with a Zeiss M10 electron microscope.

Immunocytochemistry

The procedure that we used allows the characterization of the fine structure of cells immunostained at the light microscopic level (Trapp and Quarles, 1982). Briefly, 1-μm semi-thin and thin sections were cut alternately. The 1-μm sections were deplasticized with a solution of sodium ethoxide/absolute ethanol followed by 0.03% hydrogen peroxide treatment. The tissue was then immunostained for MAG (1:250) by the peroxidase-antiperoxidase technique (Sternberger et al., 1970). Immunostained sections were photographed and directly compared with electron micrographs showing the same area from adjacent thin sections.

Results

Turnover of MAG and Sulfatides

The turnover rate of [^{3}H]fucose was measured in *mld* and control mice, 16 h and 6, 12, and 15 d after the intracerebral injection. In 21- and 60-d-old animals, [^{3}H]fucose in total brain homogenates showed a half-life of ~12 d for both control and *mld* mice. In control myelin the specific radioactivity of [^{3}H]fucose in MAG remained practically constant during

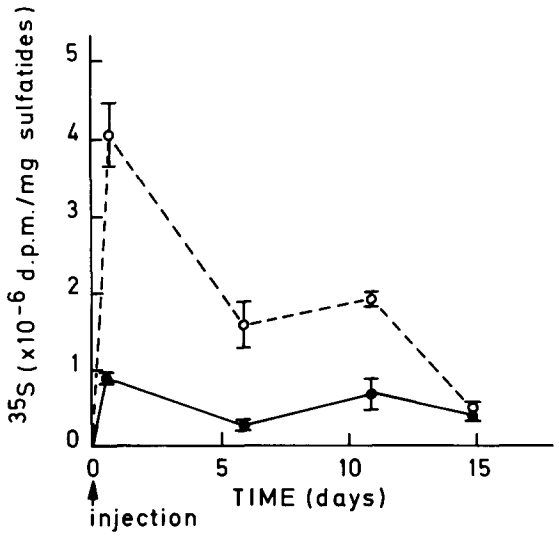

Figure 2. Metabolism of sulfatides labeled in vivo with [^{35}S]sulfate. Normal littermates (*solid circle*) and *mld* mutants (*open circle*) were injected at 21 d of age and killed after 16 h and 6, 12, and 15 d. The results expressed as specific radioactivity in dpm are the mean for three to four separate animals given with the standard error of the mean.

the study period (Fig. 1). In *mld* myelin, the rate of incorporation of [^{3}H]fucose into MAG was four times higher than in controls and the turnover of MAG was very fast, with a half-life of ~10 d in 21- and 60-d-old mutants (Fig. 1).

The turnover of ^{35}S-labeled material in total brain homogenates after intracerebral injection of [^{35}S]sodium sulfate at 21 and 60 d of age was similar for *mld* and control mice. In control myelin, [^{35}S]sulfatide specific radioactivity remained stable during the study period (Fig. 2). Control experiments showed that after separation on one-dimensional thin layer chromatography, 98% of the total radioactive sulfate present in myelin lipids was recovered in the sulfatide spots. In *mld* myelin 16 h after the injection, the specific radioactivity of [^{35}S]sulfatides was two and a half to four times higher than in controls. The turnover rate of [^{35}S]sulfatides in *mld* myelin was very fast, with a half-life of ~10 days (Fig. 2).

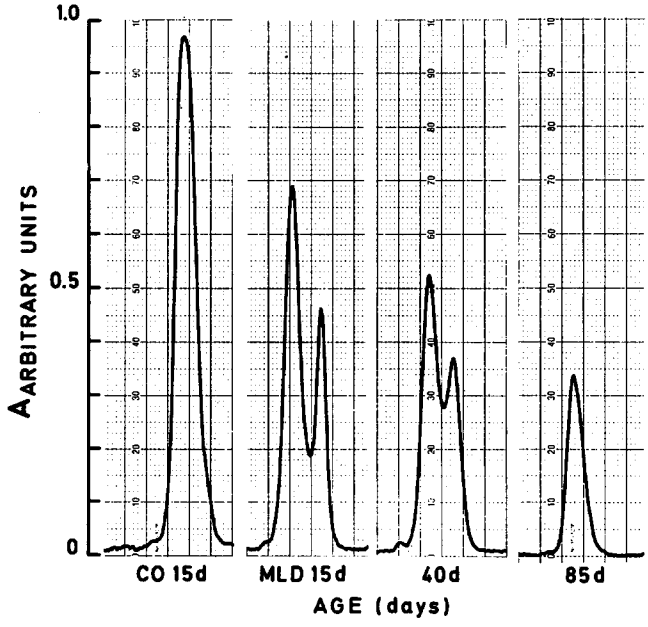

Figure 3. Densitometric scans of MAG immunoblots from 12.5% polyacrylamide slab gels. Direction of migration from the left to the right. Each well contained 50 μg of myelin protein. Autoradiographs were exposed for 5 h. CO, control.

Characterization of MAG by Electrophoretic Analysis and Immunoblotting

MAG in the spinal cord and optic nerves of control and *mld* mice was studied by electrophoresis and immunoblotting. The concentration of MAG present in the protein extract of total homogenates was reduced in *mld* mutants and decreased with age (Fig. 3). By radioimmunoassay, at 25 d of age the concentration of MAG in total brain homogenate and purified myelin of *mld* mutants was 38 and 59% of control values, respectively (Matthieu, J.-M., D. Johnson, and R. H. Quarles, manuscript in preparation).

The apparent molecular mass of MAG was 115,000 D in both control and *mld* mice. In *mld* mice, a polypeptide 10,000 D smaller than MAG was identified between 15 and 40 d, but was absent from 85-d-old mutants (Fig. 3). This lower molecular mass component reacted with two different antisera to MAG and it co-migrated with the degradation product of MAG (Matthieu et al., 1977), called dMAG by Sato et al. (1982, 1984).

In Vitro Translation of MBP, MAG, and Wolfgram Protein

Poly(A)$^{+}$ RNAs were prepared from control and *mld* brains at different ages between 18 and 85 d of age and translated in vitro in a nuclease-treated message-dependent rabbit reticulocyte lysate in the presence of L-[^{35}S]methionine. The translation products were immunoprecipitated with antisera to MBP, MAG, or Wolfgram protein, separated by electrophoresis, visualized by fluorography, and measured by densitometric scanning of fluorographs. The immunoprecipitated translation products were identified as MBP, MAG, or Wolfgram protein by the following criteria: (*a*) they reacted specifically with the relevant antiserum, (*b*) they were not precipitated by preimmune sera, and (*c*) they migrated with electrophoretic mobilities identical to those of authentic standards (data not shown). Furthermore, in the case of MBP, for which we have the purified antigen, the bands could be displaced by adding an excess of cold antigen to the immunoprecipitation mixture.

At 18 d of age, the amount of translatable messenger for MBP was drastically reduced in *mld* brains when compared with normal littermates (Fig. 4). In contrast, the amounts of translatable messenger for MAG and Wolfgram protein were increased in *mld* brains in comparison with normal littermates (Fig. 4).

MAG translation products were analyzed in *mld* and control brains at different ages between 18 and 85 d (Fig. 5). MAG was present in two different forms. The apparent molecular masses of the unprocessed polypeptide chains were 72,000 and 67,000 D, respectively (Frail and Braun, 1984). Therefore, we shall refer to these translation products as p72MAG and p67MAG. Both p72MAG and p67MAG mRNAs exhibited a sedimentation coefficient of 23S (as determined by migration on a sucrose gradient), indicating that they have similar sizes (data not shown). During develop-

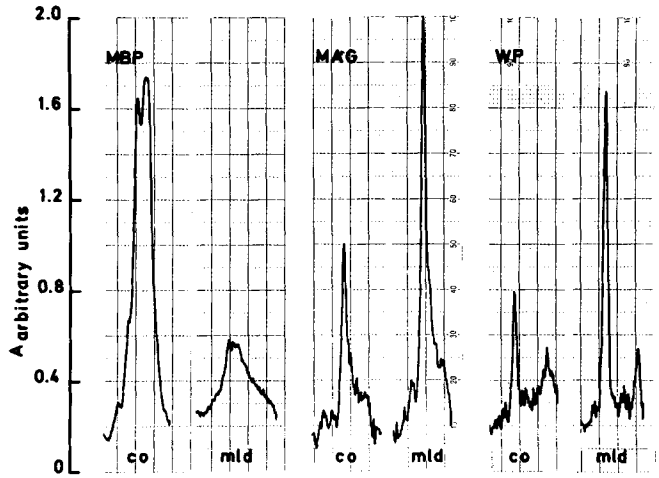

Figure 4. Densitometric scans of fluorograms of immunoprecipitated MBP, MAG, and Wolfgram protein (WP) polypeptides in normal littermate (CO, control) and *mld* mouse brains at 18 d of age. We translated 2 μg mRNA. For a given phenotype (CO or *mld*), it is not possible to compare the levels of synthesis between the three proteins, nor to make a direct correlation with the amounts of their mRNAs, because these messengers can have different translational efficiencies, and the number of methionine residues per molecule is not the same for the three proteins.

ment, the amount of translatable p72MAG mRNA decreased in control brains, whereas p67MAG mRNA, which was first detected at 25 d, reached a peak at ~40 d and then decreased (Fig. 5). In *mld* brains, the amount of p72MAG mRNA also decreased during development but the p67MAG mRNA remained at a constant level. Therefore, the ratio p72MAG/p67MAG changed during development. In control mice, the p72MAG was the predominant form of MAG at 18 and 25 d, whereas p67MAG became the major component at 40 d (Fig. 5). This shift toward the lower molecular form of MAG was delayed in *mld* brains. It occurred before 40 d in controls and after 50 d in *mld* mice (Fig. 5). These in vitro translation experiments were carried out independently in both laboratories with similar results.

Electron Microscopy and MAG Immunostaining

During active myelination (7, 15, and 25 d after birth), *mld* mutants showed morphologically and immunocytochemically altered oligodendrocytes. Approximately 70–80% of the myelin-forming glial cells were characterized by the following abnormalities (Figs. 6 *A* and 7 *A*): (*a*) dark cytoplasm, (*b*) accumulations of electron-lucent membrane-bound profiles of variable size, (*c*) atypical Golgi apparatus with dilated cisternae, and (*d*) abnormal endoplasmic reticulum (Figs. 6 *B* and 7 *A*), which was extended and often showed a whorl-like structure. However, it is interesting to note that the number of necrotic cells was not changed in *mld*

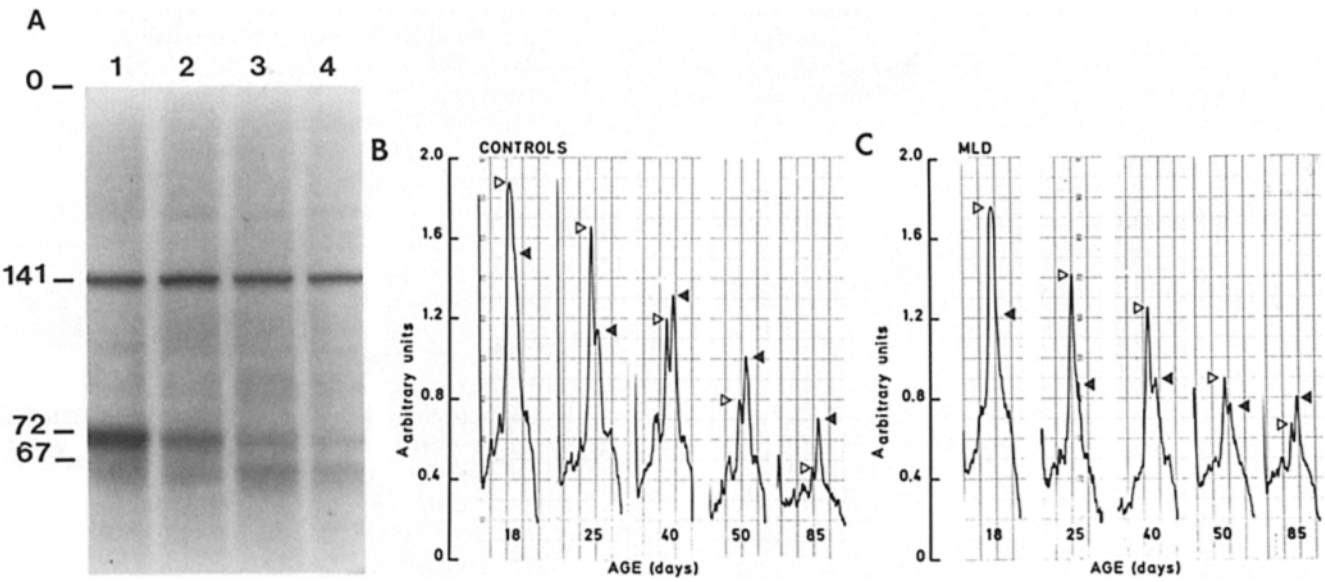

Figure 5. Fluorograms and densitometric scans of immunoprecipitated MAG polypeptides synthesized in vitro from mRNA isolated from normal littermate (controls) or *mld* mutant brains between 15 and 85 d. We translated in vitro 2 μg mRNA, immunoprecipitated the translation products with an antiserum to MAG, and analyzed them by electrophoresis and fluorography. (*A*) Fluorogram showing p72MAG and p67MAG from control brains at 18, 25, 40, and 50 d of age (lane *1–4*); 0, origin of migration. A high molecular mass (141-kD) peptide was also identified, depending on the antiserum used. The molecular mass and the intensity of labeling of this peptide remained unchanged through development and served as an internal standard. (*B* and *C*) Densitometric scans of fluorograms of immunoprecipitated p72MAG (*open arrowhead*) and p67MAG (*solid arrowhead*). The amounts of synthesized proteins, as determined by TCA immunoprecipitation, were equalized between age groups within each phenotype, controls (*B*) and *mld* (*C*). It is therefore possible to compare the level of MAG synthesis between ages within each phenotype only. It is not possible to compare the intensity of the MAG signals in terms of amounts of mRNA because: (*a*) as mentioned in the Discussion, these two polypeptides possibly contain different numbers of methionine residues, and (*b*) the two different messages may have different translational efficiencies. For a given protein, however, the amount of immunoprecipitated protein correlates well with the level of its own mRNA.

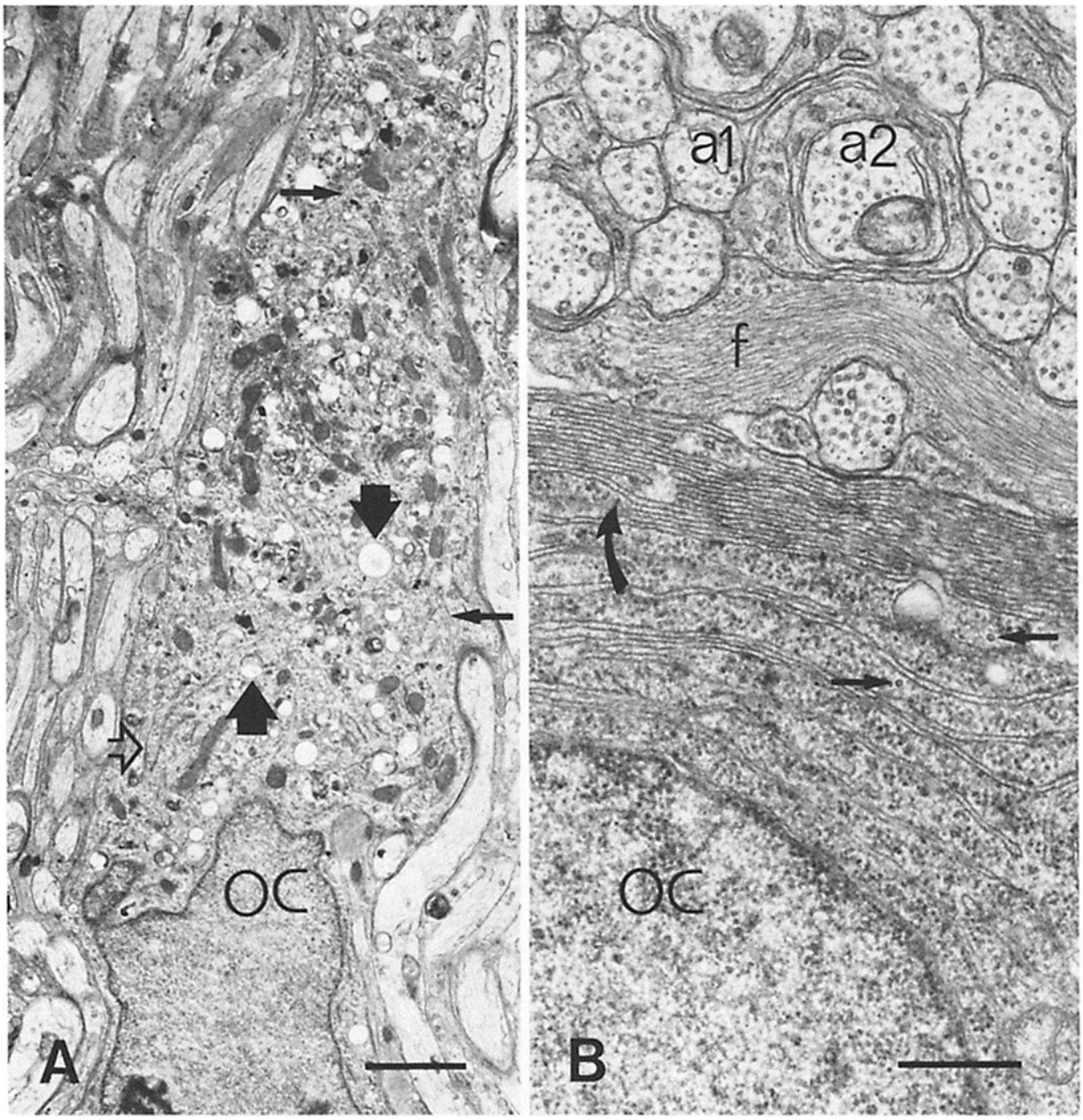

Figure 6. Electron micrographs of optic nerves of *mld* mutant mice at 15 d after birth. (*A*) Overall appearance of an abnormal oligodendrocyte (*OC*), showing a light nucleus and a relatively dark cytoplasm. Note the presence of normal mitochondria, endoplasmic reticulum (*large open arrow*), and microtubules (*small arrows*); the rough endoplasmic reticulum is often in close apposition to the mitochondria. The large solid arrow points at membrane-bound electron-lucent vesicles, which also appear in clusters. Typical features of an oligodendrocyte can be identified in the figure: light nucleus, dark cytoplasm–containing microtubules, and absence of gliofilaments. Well-defined Golgi apparatus was absent. Bar, 2 μm. (*B*) High magnification electron micrograph, which shows part of an oligodendrocyte (*OC*), an astrocytic process containing gliofilaments (*f*), naked axons (*a1*), and axons (*a2*) that are ensheathed by an uncompacted oligodendrocyte process. This oligodendrocyte shows a complex of smooth and rough endoplasmic reticulum. A sort of transition from rough to smooth endoplasmic reticulum is indicated by a curbed arrow. Microtubules in cross section are present (*small arrow*). Bar, 0.5 μm.

tissue when compared with the age-matched controls, which showed normal oligodendrocytes with their typical morphological characteristics. Furthermore, gliosis and macrophage infiltration was not present in *mld* tissue, confirming previous observations made in shiverer, the *mld* allele (Bird et al., 1978).

Adjacent semi-thin sections of *mld* (Fig. 7 *B*) and control tissue (Fig. 7 *C*) of 15-d-old animals were immunostained. The optic nerve of the mutants showed large accumulations of immunoprecipitates within the cytoplasm of these oligodendrocytes (Fig. 7 *B*, right and left arrows). The pattern of immunostaining corresponded well with the areas on the electron micrographs (Fig. 7 *A*), in which there were accumulations of membrane-bound profiles and abnormal formations of the endoplasmic reticulum. MAG-immunostained cells were clearly identified by electron microscopy

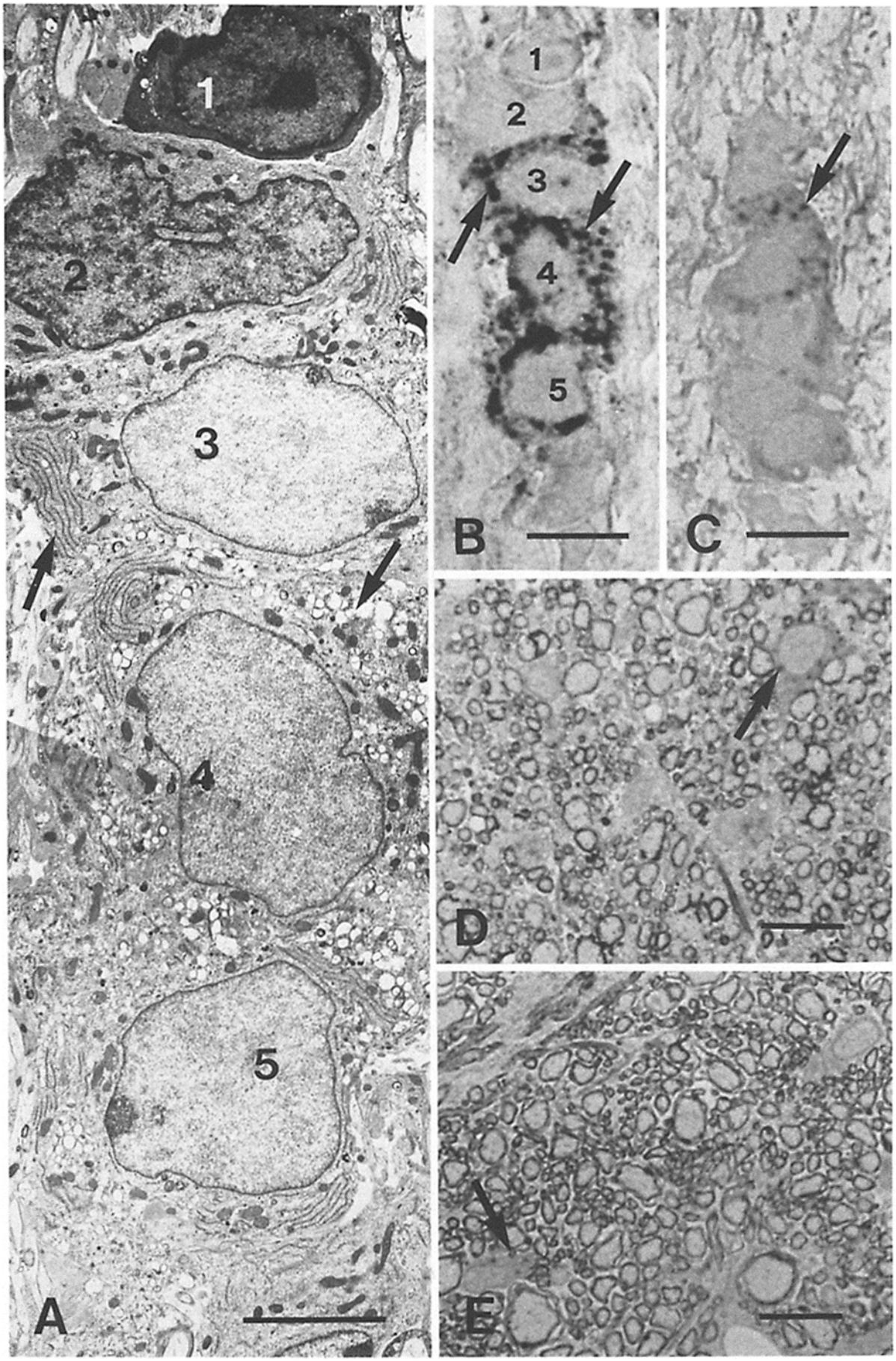
1
2
3
4
5
A
1
2
3
4
5
B
C
D
E

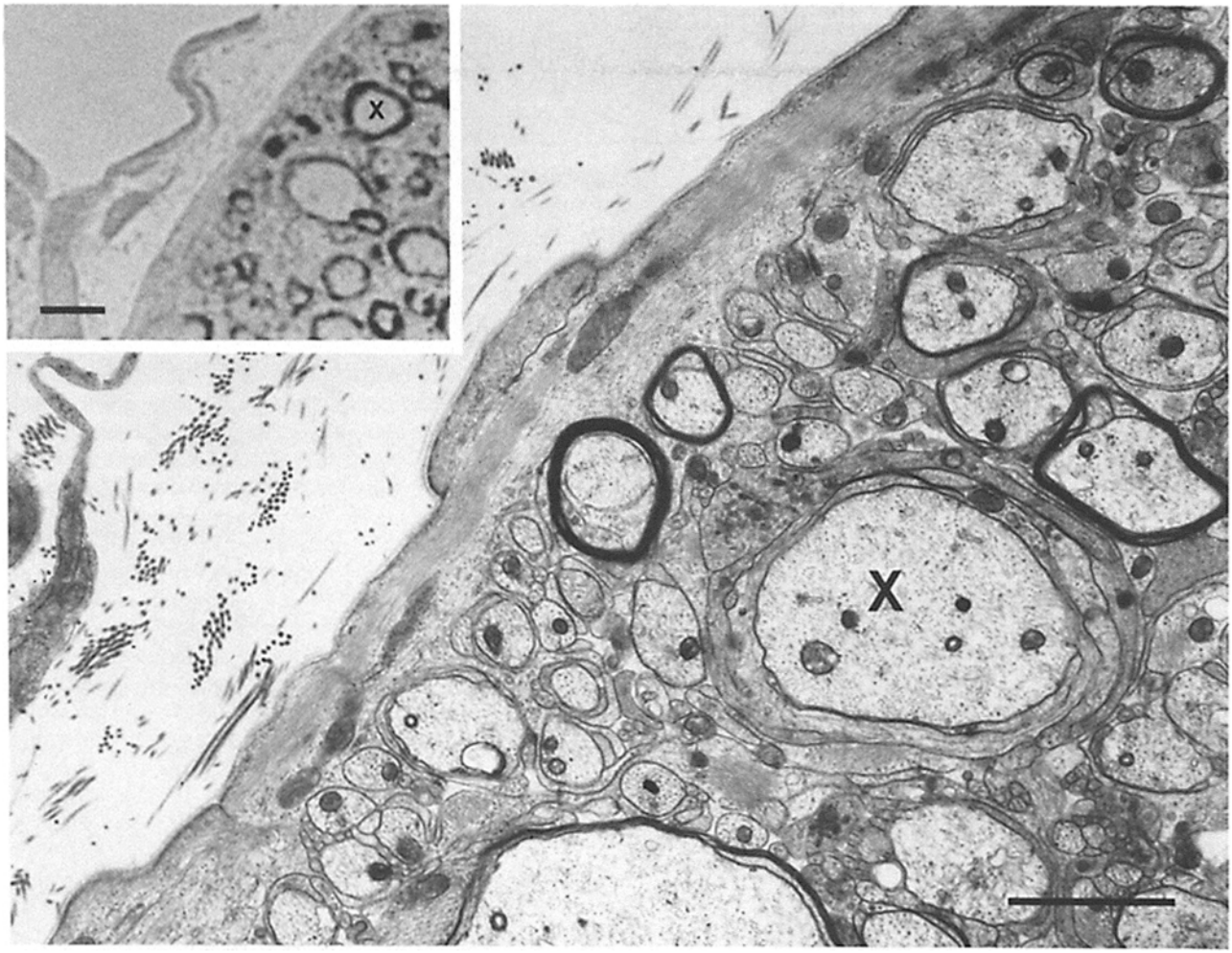

Figure 8. Electron- and light (*inset*) micrographs of adjacent thin and semi-thin sections of the cervical spinal cord from a 15-d-old *mld*. The electron micrograph shows an axon (X) that is surrounded by an oligodendrocyte process forming loose myelin. The semi-thin section is immunostained for MAG. Accumulation of immunoprecipitates are localized between these loose, uncompacted myelin membranes. Bar, 2 μm (*inset*, 4 μm).

as oligodendrocytes. Moreover, as reported previously (Matthieu and Omlin, 1984), these cells were negative for glial fibrillary acidic protein antiserum, a marker of astrocytes. At this stage, many axons were ensheathed by oligodendrocyte processes, which formed a loose sheath. Within these loops many longitudinal profiles of microtubules and vesicular structures were present (Fig. 8). The adjacent semi-thin section immunostained for MAG revealed intense immunoprecipitates, which corresponded to loose myelin (Fig. 8, inset).

At 85 d after birth, the myelination of optic nerves and cervical spinal cord in normal controls was complete. Immunostained sections of this tissue showed oligodendrocytes with granular, dot-like immunoreaction product for MAG (Fig. 7 *E*, arrow) similar to that of premyelinating stages (e.g., Fig. 7 *C*, arrow). Furthermore, a narrow ring of immunostaining was visible around axons. The age-matched *mld* (Fig. 7 *D*) showed a very similar pattern of immunostaining for MAG to that of the controls. Small granules of reaction product

Figure 7. Electron (*A*) and light micrographs (*B–E*) of optic nerves (*A–C*) and spinal cord (*D* and *E*) of *mld* mutant mice at 15 d (*A* and *B*) and 85 d (*D*) after birth, and age-matched control animals (*C* and *E*). All light micrographs of 1-μm thin sections (*B–E*) show immunostaining for MAG. (*A*) This row of interfascicular glia is composed of five cells (*1–5*), which show abnormal formations of rough endoplasmic reticulum (*left arrow*). Accumulations of membrane-bound vacuoles are also present in the cytoplasm of these oligodendrocytes (*right arrow, cells 3–5*). Bar, 5 μm. (*B*) 1-μm section immunostained for MAG adjacent to the thin section of *A*. The same row of interfascicular glia (*cells 1–5*) is shown. Accumulations of intense immunoprecipitates (*arrows*) within the cytoplasm of oligodendrocytes (*3–5*) match with the abnormal structures described in *A*. Bar, 10 μm. (*C*) Immunostained interfascicular glia cell row of a control optic nerve. The immunoprecipitates (*arrow*) within the cytoplasm of these myelinating oligodendrocytes appear dot-like and were associated with normally formed Golgi regions in corresponding electron micrographs. Bar, 10 μm. (*D* and *E*) 1-μm thick sections of *mld* (*D*) and control (*E*) cervical spinal cord of 85 d-old animals immunostained for MAG. In the *mld* tissue the staining is irregular but the intense accumulations of reaction product observed in young mice are no longer present. The pattern of staining in oligodendrocyte cell bodies is similar to age-matched controls (*arrows*). Bar, 10 μm.

were located in the cytoplasm of the oligodendrocytes (Fig. 7 *D*, arrow). Intense accumulations of immunoprecipitates in the oligodendrocytes were very rare. Furthermore, most of the axons were surrounded by a ring of immunoprecipitates comparable to that of age-matched controls. However, in some axons the labeling did not surround the whole circumference; this corresponded to the electron microscopic appearance of axons, which were surrounded by an incomplete myelin sheath (Matthieu et al., 1984b).

Discussion

Instability of Myelin in the Absence of MBP

In the central nervous system of *mld* mice during the active phase of myelin formation almost no MBP can be detected (Bourre et al., 1980; Jacque et al., 1983; Matthieu et al., 1980a, 1984b). The axons are loosely wrapped by membranes that only fuse at the extracellular sites forming the intraperiod line, and the major dense line that normally contains MBP (Golds and Braun, 1976; Omlin et al., 1982; Poduslo and Braun, 1975) is missing (Bourre et al., 1980; Matthieu et al., 1980, 1984b). At a time when the active phase of myelin deposition is already completed in controls, the MBP concentration continues to increase in *mld* myelin with the concomitant appearance of the major electron-dense line and better compaction of the myelin lamellae (Matthieu et al., 1984b). Since MBP seems to play a key role in the formation of the compact structure of central nervous system myelin, one could speculate that it is involved in the stability of the multilayered structure. Several pieces of evidence demonstrate that the uncompacted myelin lamellae in the *mld* brain are unstable. (*a*) The presence of increased levels of cholesterol esters in the brain of 25-d-old *mld* mice shows that myelin is degraded as in demyelinating disorders (Norton and Cammer, 1984). (*b*) In normal conditions, myelin proteins and lipids have extremely slow turnover rates (Benjamins and Smith, 1984). This was confirmed in the present study for MAG and sulfatides in myelin of control mice. In contrast, in *mld* myelin, both MAG and sulfatides were turned over very rapidly. (*c*) The degradation form of MAG (Matthieu et al., 1977), dMAG (Sato et al., 1982, 1984) was found in *mld* optic nerve and spinal cord when myelin is uncompacted and its MBP content drastically reduced. As reported previously (Bird et al., 1978), there was no morphological sign of massive demyelination: no phagocytosed myelin profiles, no macrophage infiltration or gliosis. This indicates a subtle myelin destruction only detected by the fast turnover rate of myelin components and by the presence of dMAG and cholesterol esters. At 85 d of age when the major dense line was present and the concentration of MBP increased, no dMAG could be found.

Recent evidence indicates that MBP is synthesized in *mld* at a very low but constant level during development (Roch, J.-M., manuscript in preparation). During the active phase of myelin formation, large amounts of membranes are produced by the oligodendrocyte, but the very low amounts of MBP are insufficient to compact the multilayered structure that then undergoes degradation. After the peak of rapid myelination is terminated, the low amounts of MBP synthesized are adequate to form the major electron-dense line and the thin myelin sheath wrapped around the axons is better compacted (Matthieu and Omlin, 1984; Matthieu et al., 1984b). In these adult mutants, dMAG is absent. This is the first direct demonstration of the role of MBP for the compaction and stability of myelin in the central nervous system.

Metabolism of Oligodendrocytes

At the electron microscopic level, the oligodendrocytes in young *mld* mice showed an accumulation of vacuolar profiles of different sizes, numerous microtubules, prominent Golgi complexes with dilated cisternae, and abnormal formation of the rough endoplasmic reticulum. Similar findings were reported by others in *mld* (Shen et al., 1985) and in shiverer mice (Inoue et al., 1983; Privat et al., 1979). This indicates an accumulation of various materials, resulting in degradation of these organelles and the formation of a lysosomal system for disposing of them. Once the concentration of MBP increases in *mld* myelin and the multilayered sheath becomes better compacted, such abnormal oligodendrocytes are rare (Matthieu and Omlin, 1984).

Previous work from this laboratory has shown that the developmental pattern of myelin lipid-synthesizing enzymes and the lipid composition of myelin is normal in *mld* mutants (Matthieu, J.-M., manuscript in preparation). Furthermore, the in vitro synthesis of two intrinsic myelin proteins present in compact myelin is not impaired in *mld* nerves (Matthieu et al., 1984). Therefore, the genetic program for myelin formation appears to be intact in the *mld* mutation and the myelin deficit seems to be secondary to the lack of MBP, which, according to our findings, appears to be responsible for the stability of the myelin sheath.

Recent work indicates that the timing of myelin gene expression is independent of continuous neuronal influence (Zeller et al., 1985) and that oligodendrocytes in culture can form compact myelin in the absence of neurons (Bradel and Prince, 1983; Guentert-Lauber et al., 1985). What remains unknown is the mechanism that turns down the synthesis of myelin components in vivo when the period of myelin thickening is completed. The present study seems to give a clue to this question. This mechanism could involve the discontinuation of an activating factor or the appearance of an inhibiting factor. In any case, this mechanism is likely to act on gene transcription, since the amounts of MBP mRNA and MAG mRNA decrease during development of normal mice (Frail and Braun, 1984; Zeller et al., 1984). In *mld* brains, the high levels of messenger for MAG and the Wolfgram protein, two proteins enriched in uncompacted myelin sheath and paranodal loops (Matthieu et al., 1973), indicate that this putative regulation signal did not reach the oligodendrocyte transcription apparatus. This hypothesis is supported by observations in other dysmyelinating mutants and does not seem to be restricted to a defect of MBP synthesis. For example, inappropriately high levels of MBP gene expression were reported in jimpy mice (Carnow et al., 1984), where the mutation affects the proteolipid protein structural gene (Dautigny et al., 1986; Gardinier et al., 1986). Furthermore, in a canine dysmyelinating mutant dog (Inuzuka et al., 1986), abnormalities were observed in oligodendrocytes similar to the ones we report here with accumulation of MAG. All of these mutants seem to be affected by a secondary defect in the regulation of myelin protein synthesis.

In *mld* mutants, the synthesis of at least two myelin-related components, MAG and the Wolfgram protein, would avoid

regulation as long as the myelin sheath is not compacted. It is likely that the synthesis of all myelin components are not under the same regulatory mechanism. The developmental shift of MAG towards a slightly lower molecular mass observed in rodents (Matthieu et al., 1974, 1975; Quarles et al., 1973) and the differences in the expression of its two molecular forms observed by Frail and Braun (1984) and in this study, support this view. Although p72MAG and p67MAG differ only by an additional sequence in the high molecular mass form (Frail and Braun, 1984), it is not known how many, if any, methionine residues this sequence contains. Clearly, the presence of methionine residues in this sequence would influence the estimation of the relative amounts of these two forms of MAG, with p72MAG being somewhat overestimated relative to p67MAG. This makes determination of the precise timing of the switch between the two forms, in the normal mouse, difficult. However, the fact remains that this switch is significantly delayed in the *mld* mouse. The prolonged predominance of the large form in the *mld* mutants could indicate a preferential localization in the uncompacted myelin sheath. In the shiverer mutant, which is allelic with the *mld* mouse (Lachapelle et al., 1980), the ratio between the two forms of MAG studied in immature and adult animals was normal (Frail and Braun, 1985). Nevertheless, a delayed change in the ratio p72MAG/p67MAG during shiverer development could have remained unnoticed, since only 15-d-old and adult mice were investigated. The function of one of the Wolfgram proteins that is identical to the myelin enzyme 2',3'-cyclic nucleotide 3'-phosphohydrolase (Drummond and Dean, 1980; Sprinkle et al., 1980), as well as that of MAG, is still unknown. Nevertheless, it is of interest that large amounts of the former (Matthieu et al., 1984b) and heavy immunostaining of the latter (Matthieu and Omlin, 1985) are present in uncompacted myelin sheath from 25-d-old *mld* mice. This implies that these two components have an important function in the initial stages of myelination, and, as suggested by Frail and Braun (1984), this function would no longer be necessary in the latter stages of myelination, or may even become incompatible, as indicated by our present data in the *mld* mutants.

We would like to thank Professor Barry Cooper (National Institute of Neurological and Communicative Disorders and Stroke, National Institutes of Health, Bethesda, MD) for valuable comments on the manuscript, Dr. Helga Ginalski-Winkelmann and Dr. Olivier Reymond for help with some of the experiments. We express our gratitude to Dr. David Johnson and Richard H. Quarles (New York State College of Veterinary Medicine, Cornell University, Ithaca, NY) for the determinations of MAG by radioimmunoassay. The technical advice of Ms. Marianne Brown-Luedi is acknowledged. We are grateful to Ms. Nathalie Eschmann and Christine Roulier for excellent technical assistance.

This work was supported by grants (3.447.83 and 3.142.85) from the Swiss National Science Foundation, the Medical Research Council of Canada, and the Multiple Sclerosis Societies of Canada and Switzerland.

Received 11 April 1986, and in revised form 10 September 1986.

References

Almazan, G., H. Ginalski-Winkelmann, and J.-M. Matthieu. 1983. Myelin metabolism in a dysmyelinating mutant mouse (*mld*). *Trans. Am. Soc. Neurochem.* 14:129. (Abstr.)

Benjamins, J. A., and M. E. Smith. 1984. Metabolism of Myelin. *In* Myelin. P. Morell, editor. Plenum Publishing Corp., New York. 225–258.

Bird, T. D., D. F. Farrell, and S. M. Sumi. 1978. Brain lipid composition of the shiverer mouse: (genetic defect in myelin development). *J. Neurochem.* 31:387–391.

Bourre, J. M., C. Jacque, A. DeLassalle, J. Nguyen-Legros, O. Dumont, F. Lachapelle, M. Raoul, C. Alvarez, and N. Baumann. 1980. Density profile and basic protein measurements in the myelin range of particulate material from normal developing mouse brain and from neurological mutants (*Jimpy; Quaking; Trembler; Shiverer* and its mld allele) obtained by zonal centrifugation. *J. Neurochem.* 35:458–464.

Bradel, E., and F. Prince. 1983. Cultured neonatal rat oligodendrocytes elaborate myelin membrane in the absence of neurons. *J. Neurosci. Res.* 9:381–392.

Braun, P. E. 1984. Molecular organization of myelin. *In* Myelin. P. Morell, editor. Plenum Publishing Corp., New York. 97–116.

Campagnoni, A. T., C. W. Campagnoni, J.-M. Bourre, C. Jacque, and N. Baumann. 1984. Cell-free synthesis of myelin basic proteins in normal and dysmyelinating mutant mice. *J. Neurochem.* 42:733–739.

Carnow, T. B., J. H. Carson, S. W. Brostoff, and E. L. Hogan. 1984. Myelin basic protein gene expression in quaking, jimpy, and myelin synthesis-deficient mice. *Dev. Biol.* 106:38–44.

Dautigny, A., M.-G. Mattei, D. Morello, P. M. Alliel, D. Pham-Dinh, L. Amar, D. Arnaud, D. Simon, J.-F. Mattei, J.-L. Guenet, P. Jollès, and P. Avner. 1986. The structural gene coding for myelin-associated proteolipid protein is mutated in *jimpy* mice. *Nature (Lond.).* 321:867–869.

Doolittle, D. P., and K. M. Schweikart. 1977. Myelin deficient, a new neurological mutant in the mouse. *J. Hered.* 68:331–332.

Drummond, R. J., and G. Dean. 1980. Comparison of 2',3'-cyclic nucleotide 3'-phosphodiesterase and the major component of Wolfgram protein WI. *J. Neurochem.* 35:1155–1165.

Dupouey, P., C. Jacque, J. M. Bourre, F. Cesselin, A. Privat, and N. Baumann. 1979. Immunochemical studies of a myelin basic protein in Shiverer mouse devoid of major dense line of myelin. *Neurosci. Lett.* 12:113–118.

Folch, J., M. Lees, and G. H. Sloane-Stanley. 1957. A simple method for the isolation and purification of total lipids from animal tissue. *J. Biol. Chem.* 266:497–509.

Frail, D. E., and P. E. Braun. 1984. Two developmentally regulated messenger RNAs differing in their coding region may exist for the myelin-associated glycoprotein. *J. Biol. Chem.* 259:14857–14862.

Frail, D. E., and P. E. Braun. 1985. Abnormal expression of the myelin-associated glycoprotein in the central nervous system of dysmyelinating mutant mice. *J. Neurochem.* 45:1071–1075.

Gardinier, M. V., P. L. Deininger, and W. B. Macklin. 1986. Myelin proteolipid mRNA in normal and jimpy brain development. *Trans. Am. Soc. Neurochem.* 17:109. (Abstr.)

Ginalski-Winkelmann, H., T. V. Waehneldt, S. R. Cohen, and J.-M. Matthieu. 1982. Density distribution of 2',3'-cyclic nucleotide 3'-phosphodiesterase and myelin proteins in particulate material from myelin deficient (*mld*) mutant and control brains. *Neurochem. Int.* 4:67–71.

Ginalski-Winkelmann, H., G. Almazan and J.-M. Matthieu. 1983. In vitro myelin basic protein synthesis in the PNS and CNS of myelin deficient (*mld*) mutant mice. *Brain Res.* 277:386–388.

Golds, E. E., and P. E. Braun. 1976. Organization of membrane proteins in the intact myelin sheath. *J. Biol. Chem.* 251:4729–4735.

Guentert-Lauber, B., F. Monnet-Tschudi, F. X. Omlin, P. Favrod, and P. Honegger. 1985. Serum-free aggregate cultures of rat CNS glial cells: biochemical, immunocytochemical and morphological characterization. *Dev. Neurosci.* 7:33–44.

Inoue, Y., K. Inoue, T. Terashima, K. Mikoshiba, and Y. Tsukada. 1983. Developmental changes of oligodendroglia in the posterior funiculus of "Shiverer" mutant mouse spinal cord, with special reference to myelin formation. *Anat. Embryol.* 168:159–171.

Inuzuka, T., I. D. Duncan, and R. H. Quarles. 1986. Myelin proteins in the CNS of 'shaking pups'. *Dev. Brain Res.* 27:43–50.

Jacque, C., A. DeLassalle, M. Raoul, and N. Baumann. 1983. Myelin basic protein deposition in the optic and sciatic nerves of dysmyelinating mutants quaking, jimpy, trembler, mld, and shiverer during development. *J. Neurochem.* 41:1335–1340.

Johnson, D., R. H. Quarles, and R. O. Brady. 1982. A radioimmunoassay for the myelin-associated glycoprotein. *J. Neurochem.* 39:1356–1362.

Kean, E. L. 1968. Rapid sensitive spectrophotometric method for quantitative determination of sulfatides. *J. Lipid Res.* 9:319–327.

Kimura, M., H. Inoko, M. Katsuki, A. Ando, T. Sato, T. Hirose, H. Takashima, S. Inayama, H. Okano, K. Takamatsu, K. Mikoshiba, Y. Tsukada, and I. Watanabe. 1985. Molecular genetic analysis of myelin-deficient mice: *shiverer* mutant mice show deletion in gene(s) coding for myelin basic protein. *J. Neurochem.* 44:692–696.

Kirschner, D. A., A. L. Ganser, and D. L. D. Caspar. 1984. Diffraction studies of molecular organization and membrane interactions in myelin. 2nd ed. *In* Myelin. P. Morell, editor. Plenum Publishing Corp., New York. 51–95.

Kraus-Ruppert, R., A. Wildbolz, J.-M. Matthieu, and N. Herschkowitz. 1972. The late form of metachromatic leukodystrophy. I. A histochemical and neurochemical study. *J. Neurol. Sci.* 17:373–381.

Lachapelle, F., C. de Baecque, C. Jacque, J.-M. Bourre, A. Delassalle, D. Doolittle, J. J. Hauw, and N. Baumann. 1980. Comparison of morphological and biochemical defects of two probably allelic mutations of the mouse myelin deficient (mld) and shiverer (shi). *In* Neurological Mutations Affecting Myelination. INSERM Symposium No. 14. N. Baumann, editor. Elsevier/North-Holland, New York. 27–32.

Laemmli, U. K. 1970. Cleavage of structural proteins during the assembly of the head of bacteriophage T4. *Nature (Lond.).* 227:680–685.

Lowry, O. H., N. J. Rosebrough, A. L. Farr, and R. J. Randall. 1951. Protein measurement with the folin phenol reagent. *J. Biol. Chem.* 193:265–275.

Maniatis, T., E. F. Fritsch, and J. Sambrook. 1982. Molecular Cloning. A Laboratory Manual. Cold Spring Harbor Laboratory, Cold Spring Harbor, New York. 187–199 and 310.

Matthieu, J.-M., R. H. Quarles, R. O. Brady, and H. deF. Webster. 1973. Variation of proteins, enzyme markers and gangliosides in myelin subfractions. *Biochim. Biophys. Acta.* 329:305–317.

Matthieu, J.-M., R. O. Brady, and R. H. Quarles. 1974. Developmental change in a myelin-associated glycoprotein: a comparative study in rodents. *Dev. Biol.* 37:146–152.

Matthieu, J.-M., R. O. Brady, and R. H. Quarles. 1975. Change in a myelin-associated glycoprotein in rat brain during development: metabolic aspects. *Brain Res.* 86:55–65.

Matthieu, J.-M., B. Koellreutter, and M.-L. Joyet. 1977. Changes in CNS myelin proteins and glycoproteins after in situ autolysis. *Brain Res. Bull.* 2:15–21.

Matthieu, J.-M., H. Ginalski, R. L. Friede, S. R. Cohen, and D. P. Doolittle. 1980a. Absence of myelin basic protein and major dense line in CNS myelin of the mld mutant mouse. *Brain Res.* 191:278–283.

Matthieu, J.-M., J. Reigner, E. Costantino-Ceccarini, J.-M. Bourre, and M. Rutti. 1980b. Abnormal sulfate metabolism in a hereditary demyelinating neuropathy. *Brain Res.* 200:457–465.

Matthieu, J.-M. 1981. Glycoproteins associated with myelin in the central nervous system. *Neurochem. Int.* 3:355–363.

Matthieu, J.-M., H. Ginalski-Winkelmann, and C. Jacque. 1981. Similarities and dissimilarities between two myelin deficient mutant mice, Shiverer and *mld*. *Brain Res.* 214:219–222.

Matthieu, J.-M., H. Ginalski-Winkelmann, D. Johnson, P. Bürgisser, R. H. Quarles, J. F. Poduslo, and R. Krstić. 1982. Composition and metabolism of CNS myelin from young *mld* mice. *Trans. Am. Soc. Neurochem.* 13:215. (Abstr.)

Matthieu, J.-M., and F. X. Omlin. 1984. Murine leukodystrophies as tools to study myelinogenesis in normal and pathological conditions. *Neuropediatrics.* 15(Suppl.):37–52.

Matthieu, J.-M., G. Almazan, and T. V. Waehneldt. 1984a. Intrinsic myelin proteins are normally synthesized in vitro in the myelin-deficient (*mld*) mutant mouse. *Dev. Neurosci.* 6:246–250.

Matthieu, J.-M., F. X. Omlin, H. Ginalski-Winkelmann, and B. J. Cooper. 1984b. Myelination in the CNS of *mld* mutant mice: comparison between composition and structure. *Dev. Brain Res.* 13:149–158.

Matthieu, J.-M., and F. X. Omlin. 1985. Myelin-associated glycoprotein in the CNS of myelin-deficient (*mld*) mutant mice. An immunochemical and immunocytochemical study. *Trans. Am. Soc. Neurochem.* 16:139. (Abstr.)

Matthieu, J.-M., T. V. Waehneldt, and N. Eschmann. 1986. Myelin-associated glycoprotein and myelin basic protein are present in central and peripheral nerve myelin throughout phylogeny. *Neurochem. Int.* 8:521–526.

Norton, W. T., and S. E. Poduslo. 1973. Myelination in rat brain: method of myelin isolation. *J. Neurochem.* 21:749–758.

Norton, W. T., and W. Cammer. 1984. Isolation and characterization of myelin. *In* Myelin. P. Morell, editor. Plenum Publishing Corp., New York. 147–195.

Omlin, F. X., H. deF. Webster, C. G. Palkovits, and S. R. Cohen. 1982. Immunocytochemical localization of basic protein in major dense line regions of central and peripheral myelin. *J. Cell Biol.* 95:242–248.

Omlin, F. X., and J.-M. Matthieu. 1984. Myelin-associated glycoprotein (MAG): immunocytochemical localization in both oligodendrocytes and myelin loops of myelin deficient (*mld*) mutant mice. *Soc. Neurosci. Abstr.* 10:949.

Poduslo, J. F., and P. E. Braun. 1975. Topographical arrangement of membrane proteins in the intact myelin sheath. *J. Biol. Chem.* 250:1099–1105.

Privat, A., C. Jacque, J.-M. Bourre, P. Dupouey, and N. Baumann. 1979. Absence of the major dense line in myelin of the mutant mouse "shiverer". *Neurosci. Lett.* 12:107–112.

Quarles, R. H., J. L. Everly, and R. O. Brady. 1973. Myelin-associated glycoprotein: a developmental change. *Brain Res.* 58:506–509.

Quarles, R. H., G. R. Barbarash, and T. D. MacIntosh. 1985. Methods for the identification and characterization of glycoproteins in central and peripheral myelin. *In* Research Methods in Neurochemistry. Vol. 6. N. Marks and R. Rodnight, editors. Plenum Publishing Corp., New York. 303–357.

Roach, A., K. Boylan, S. Horvath, S. B. Prusiner, and L. E. Hood. 1983. Characterization of cloned cDNA representing rat myelin basic protein: absence of expression in brain of shiverer mutant mice. *Cell.* 34:799–806.

Roch, J.-M., M. Brown-Luedi, B. J. Cooper, and J.-M. Matthieu. 1986. Mice heterozygous for the *mld* mutation have intermediate levels of myelin basic protein mRNA and its translation products. *Mol. Brain Res.* In press.

Sato, S., R. H. Quarles, and R. O. Brady. 1982. Susceptibility of the myelin-associated glycoprotein and basic protein to a neutral protease in highly purified myelin from human and rat brain. *J. Neurochem.* 39:97–105.

Sato, S., K. Yanagisawa, and T. Miyatake. 1984. Conversion of myelin-associated glycoprotein (MAG) to a smaller derivative by calcium activated neutral protease (CANP)-like enzyme in myelin and inhibition by E-64 analogue. *Neurochem. Res.* 9:629–635.

Shen, X.-Y., S. Billings-Gagliardi, R. L. Sidman, and M. K. Wolf. 1985. Myelin deficient (shi^{mld}) mutant allele: morphological comparison with shiverer (*shi*) allele on a B6C3 mouse stock. *Brain Res.* 360:235–247.

Sprinkle, T. J., M. R. Wells, F. A. Garver, and D. B. Smith. 1980. Studies on the Wolfgram high molecular weight CNS myelin proteins: relationship to 2′,3′-cyclic nucleotide 3′-phosphodiesterase. *J. Neurochem.* 35:1200–1208.

Sternberger, L. A., P. H. Hardy, J. J. Cuculis, and H. E. Meyer. 1970. The unlabeled antibody-enzyme method of immunohistochemistry. Preparation and properties of soluble antigen-antibody complex (horseradish peroxidase-antihorseradish peroxidase) and its use in identification of spirochetes. *J. Histochem. Cytochem.* 18:315–333.

Towbin, H., T. Staehelin, and J. Gordon. 1979. Electrophoretic transfer of proteins from polyacrylamide gels to nitrocellulose sheets: procedure and some applications. *Proc. Natl. Acad. Sci. USA.* 76:4350–4354.

Trapp, B. D., and R. H. Quarles. 1982. Presence of the myelin-associated glycoprotein correlates with alterations in the periodicity of peripheral myelin. *J. Cell Biol.* 92:877–882.

Waehneldt, T. V., J. Malotka, N. J. Karin, and J.-M. Matthieu. 1985. Phylogenetic examination of vertebrate central nervous system myelin proteins by electro-immunoblotting. *Neurosci. Lett.* 57:97–102.

Zeller, N. K., M. J. Hunkeler, A. T. Campagnoni, J. Sprague, and R. A. Lazzarini. 1984. Characterization of mouse myelin basic protein messenger RNAs with a myelin basic protein cDNA clone. *Proc. Natl. Acad. Sci. USA.* 81:18–22.

Zeller, N. K., T. N. Behar, M. E. Dubois-Dalcq, and R. A. Lazzarini. 1985. The timely expression of myelin basic protein gene in cultured rat brain oligodendrocytes is independent of continuous neuronal influences. *J. Neurosci.* 5:2955–2962.